Interaction between Human CD2 and CD58 Involves the Major β Sheet Surface of each of Their Respective Adhesion Domains

By Antonio R. N. Arulanandam,*‡ Alexander Kister,*‡ Malcolm J. McGregor,¶ Daniel F. Wyss,§ Gerhard Wagner,§ and Ellis L. Reinherz*‖

*From the *Laboratory of Immunobiology, Dana-Farber Cancer Institute and the Departments of ‡Pathology, §Biological Chemistry and Molecular Pharmacology, and ‖Medicine, Harvard Medical School, Boston, Massachusetts 02115; and ¶Procept, Inc., Cambridge, Massachusetts 02139*

Summary

The CD58 binding site on human CD2 was recently shown by nuclear magnetic resonance structural data in conjunction with site-directed mutagenesis to be a highly charged surface area covering ~770Å^2 on the major AGFCC'C'' face of the CD2 immunoglobulin-like (Ig-like) NH_2-terminal domain. Here we have identified the other binding surface of the CD2-CD58 adhesion pair by mutating charged residues shared among CD2 ligands (human CD58, sheep CD58, and human CD48) that are predicted to be solvent exposed on a molecular model of the Ig-like adhesion domain of human CD58. This site includes β strand residues along the C strand (E25, K29, and K30), in the middle of the C' strand (E37) and in the G strand (K87). In addition, several residues on the CC' loop (K32, D33, and K34) form this site. Thus, the interaction between CD2 and CD58 involves the major β sheet surface of each adhesion domain. Possible docking orientations for the CD2–CD58 molecular complex are offered. Strict conservation of human and sheep CD58 residues within the involved C and C' strands and CC' loop suggests that this region is particularly important for stable formation of the CD2–CD58 complex. The analysis of this complex offers molecular insight into the nature of a receptor-ligand pair involving two Ig family members.

The interaction of human CD2 on T lymphocytes with CD58 on the surface of antigen-presenting, epithelial, endothelial, and target cells of various types is critical for T lymphocytes to mediate their regulatory and effector functions (1–3). The adhesion domains of CD2 and CD58 facilitate the antigen recognition process by stabilizing cell–cell contact (4, 5). In addition, ligation of CD2 by CD58 or anti-CD2 mAbs provides signals via the CD2 cytoplasmic tail, thereby lowering the activation threshold for TCR triggering (6–11). CD2 also facilitates cytotoxic function of NK cells through similar mechanisms (12–14).

The membrane distal NH_2-terminal domains of human CD2 and human CD58 bind to one another with a micromolar affinity (15–17). This modest, monomeric binding activity is amplified by multimeric interaction at the cell–cell interface resulting from rapid redistribution of CD2 to the intercellular junction (5, 18). Human CD2 also interacts with sheep CD58, providing the molecular basis for the fortuitous observation that human T cells and sheep erythrocytes form aggregates, or "rosettes," in vitro (19–23). This rosetting phenomenon was used to enumerate T lymphocytes in humans long before the discovery of CD2 (20–23). Human CD2 interacts with a second structurally related human ligand, CD48 (24). However, the affinity of the CD2–CD48 interaction is 2 orders of magnitude weaker (10^{-4} M) than that of the CD2–CD58 interaction and hence, is unable to support cell adhesion in an in vitro assay (24). In the murine system, in contrast, CD48 is the only known ligand for CD2 (25). Thus, it appears that the ligands of CD2 have diverged during the evolution of humans and rodents (24).

Molecular cloning of human CD2 and CD58 indicated that their gene products are ~20% homologous at the amino acid level and suggested their structure to be Ig-like (26–30). Nuclear magnetic resonance (NMR)[1] spectroscopy and x-ray crystallographic studies confirm that both rat and human CD2 adhesion domains adopt the predicted Ig fold (31–34). Human

[1] *Abbreviations used in this paper:* aa, amino acid; NMR, nuclear magnetic resonance.

 J. Exp. Med. © The Rockefeller University Press • 0022-1007/94/11/1861/11 $2.00
Volume 180 November 1994 1861–1871

CD48 shares somewhat higher homology (~30%) with both human CD2 and CD58, implying that human CD58 may have evolved from CD48 (24, 35, 36). The human CD2 and CD58 genes are located on chromosome 1p and the CD48 gene is on 1q (36, 37). These genes are tightly linked with the ATP1A genes on chromosome 1 which have evolved by gene duplication (36–38). By inference, it is likely that duplication of a primordial gene also gave rise to the structurally related CD2, CD58, and CD48 genes (36, 38). In this regard, the human genomic organization of CD2 and CD58 is similar except for an additional exon in human CD58 which contains the alternative splice sites for the phosphatidyl-inositol (PI), linked and transmembrane forms of CD58 (39, and Wallich, R., personal communication). However, the tissue distributions of CD58, CD48, and CD2 markedly differ from one another. CD58 is ubiquitously expressed in many diverse cell types, whereas CD48 expression is restricted to leukocytes and human CD2 is limited to T and NK cells (40–42).

Site-directed mutagenesis studies based on the NMR structure of the adhesion domain of human CD2 defines the CD58 binding surface as a highly charged surface area restricted to the AGFCC'C" face of its Ig-like domain (43). An independent mutagenesis study predicated on a homology model of the human CD2 adhesion domain yields similar conclusions (44). Given these findings, it seems likely that a charged surface on the NH_2-terminal domain of human CD58 might bind to CD2. Based on this speculation and the known sequences of human CD2 ligands (human CD58, human CD48, and sheep CD58), we selected charged residues on human CD58 that are conserved among the CD2 ligands for site-directed mutagenesis. The ability of mutant CD58 molecules to bind CD2 was then analyzed and the binding site for human CD2 on CD58 was mapped. In addition, the predicted structural features shared in common by the other CD2 ligands permits us to infer how they might bind to CD2 as well.

Materials and Methods

Antibodies. TS2/9 mAb was provided by Dr. T. Springer (Center for Blood Research, Boston, MA). All other anti-CD58 mAbs used in this study were generously provided by Dr. Stefan Meuer (German Cancer Research Center, Heidelberg, Germany) (45). The CD58 heteroantisera, Rb202, was provided by Dr. Laurlee Osborn (Biogen Inc., Cambridge, MA) (17).

Site-directed Mutagenesis. A 0.8-kb CD58 cDNA fragment was excised from CDM8 (28) with XbaI and subcloned into the XbaI site of M13mp18 in order to generate site-directed mutants. Mutagenesis and subcloning of mutant CD58 cDNA molecules into the CDM8 expression vector was conducted as previously described (43). The entire adhesion domain of each variant was sequenced to exclude second-site mutations.

Transfection, Binding Analysis, and Immunofluorescence Assays. CHO cells were cultured and transfected with CD58 cDNAs as previously described (24). Stable CHO cell lines expressing mutant CD58 at copy numbers comparable or higher than wtCD58-transfected CHO cells were derived by fluorescence-activated cell sorting of the parental transfectants. For this purpose, we used a rabbit heteroantisera specific for the extracellular segment of CD58, termed RB202 (1:100 dilution) followed by staining with FITC-conjugated goat anti-rabbit Ig (Tago, Inc., Burlingame, CA). For binding studies, CHO cells expressing mutant or wtCD58 molecules were plated in triplicates at 5×10^4 cells/well in 24-well plates and analyzed for CD2 binding using ^{51}Cr-labeled Jurkat cells as previously described (24). For experiments aimed at identifying anti-CD58 mAb binding residues on human CD58, nonsaturating concentrations of mAbs (yielding between 50 and 90% of maximum fluorescence) on wtCD58-transfected CHO cells when developed using a goat anti-mouse Ig labeled with FITC (BioWhittaker, Inc., Walkersville, MD) were used to optimize sensitivity. Cell-bound immunofluorescence was determined using a FACScan® (Becton Dickinson & Co., Mountain View, CA) as described (see legend to Table 1).

Molecular Modeling of the Human CD58 Adhesion Domain. Two three-dimensional molecular models of the adhesion domain of human CD58 were developed independently, based on homology with the known three-dimensional NMR structure of the human CD2 adhesion domain (32, 33).

The first model was based on a structural alignment of human CD2, rat CD2, human CD4, human CD8, and REI Ig molecules (31–33, 46–48). This produced a sequence alignment to which the CD58 sequence was aligned. The coordinates of the main chain secondary structure regions were taken from human CD2 (average of 18 newly refined NMR structures, energy minimized). The conformations of the loops were modeled on the structure whose sequence in the loop most closely resembles that of CD58. For example, the conformation of the CC' loop was modeled on the corresponding loop in rat CD2 (involving a two-residue deletion in human CD2). The C'C" loop was formed by deleting E52 in human CD2, which is a bulge at the beginning of the C" strand, and preserving the conformation of the turn. The C"D loop was modeled on that of CD4 in order to form a salt bridge between residues R52 and D71. This salt bridge is conserved in most Ig domains, but is not present in CD2. For the FG loop, the alignment of the F and G strands means that if the strands form a β-hairpin, this puts proline 80 in the first position of a four-residue β-turn; this is unusual and introduces a conformational distortion. There is no similar loop in the above structures but one was found in the FG loop of a mouse Ig H chain constant domain (Brookhaven structure 1FAI) and this was incorporated into the model. The side chain conformations were chosen using the above structures as a guide and ensuring that no severe steric clashes were created.

In the second model, a secondary structural alignment based on human CD2 was used and the conformation of loops chosen to provide best conformity with the experimentally derived mAb and CD2 binding results. Both models were energy minimized using the Amber force field in the Discover program from Biosyn Technologies (San Diego, CA). The two CD58 models differ slightly in the alignment of the A and C" strands, and in the EF loop (data not shown). However, they are in agreement as to the alignment of the important F, G, C, and C' strands where most of the mutations are located.

Results and Discussion

Sequence Alignment of the Adhesion Domains of CD58, CD48, and CD2. The NMR studies of rat and human CD2 adhesion domains show that each adopts an Ig fold (31–33). These solution structures were confirmed and extended by x-ray crystallography analyses of the entire rat CD2 ectodomain (34). The second domain was found to be Ig-like as well and connected to the membrane-distal first domain by a flexible hinge region. Given the weak but nevertheless significant homology between the extracellular segments of human CD2

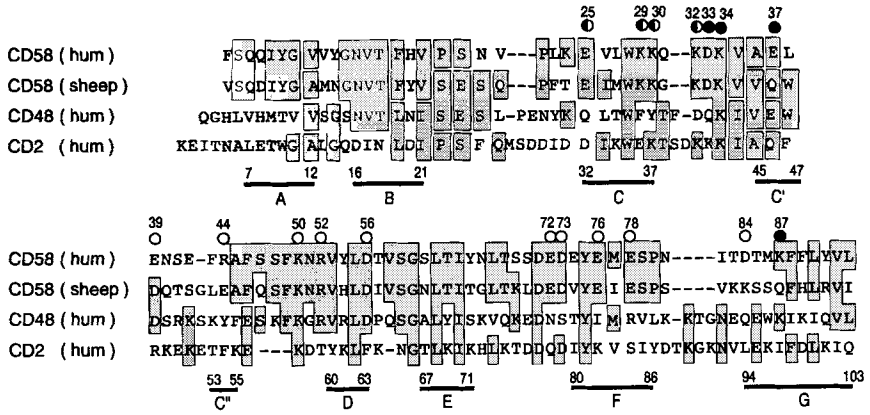

Figure 1. Alignment of amino acid sequences in the adhesion domains of CD58, CD48, and CD2. The amino acid sequences were aligned as described in Materials and Methods. The positions for the β strand and loop residues in the human CD2 adhesion domain (32, 33) are shown as defined by NMR analysis. Residues that are conserved between all sequences are boxed and shaded. CD58 residues that are involved in binding CD2 are shown in either closed circles (strong effects) or half-closed circle (partial effect). Analyzed residues not involved in binding CD2 are shown in open circles (no effect). Sheep CD58 sequence data are available from GSDB/DDBJ/EMBL/NCBI DNA under accession number D28584.

and human CD58, it is likely that CD58 also consists of two Ig-like domains (28).

The NH_2-terminal domain (amino acid [aa][1] 1–93) of CD58 has been shown to contain the CD2 binding region (17). Fig. 1 offers an alignment between human CD2 and human CD58 adhesion domains and indicates the position of the CD2 β strands as defined by NMR. The conservation of multiple key amino acid residues found in Ig domains implies that the CD58 adhesion domain adopts an Ig-fold. An invariant tryptophan (W28) in the predicted C strand is present at the same position in all known Ig supergene family members. In addition, other CD58 residues including V13, F15, V35, R52, L62, I64, D71, Y75, L90, and V92 are conserved among Ig family members (Fig. 1 and data not shown). R52 at the end of the predicted C"D loop and D71 in the predicted EF turn presumably form a salt bridge that is characteristic of most Ig molecules. This salt bridge is absent in CD2. In addition, the human CD58 adhesion domain, like the CD2 adhesion domain, also differs from conventional Ig domains in lacking two cysteine residues which form an intradomain disulfide bond in almost all Ig domains (28–30). Valine (V17) at the end of the predicted CD58 B strand and methionine (M77) at the predicted F strand presumably function in lieu of the cysteine residues to mediate hydrophobic contacts (Fig. 1). In this regard, replacement of the corresponding hydrophobic residues on rat CD2 in the B and F strands by cysteines through site-directed mutagenesis showed that a disulfide bond forms at this position (49). Hydrophobic residue (V13) is located near the start of the B strand and Y75 is located two residues NH_2-terminal to M77, near the beginning of the F strand. These hydrophobic residues are hallmarks of Ig domains and form part of the hydrophobic core of the Ig domain (30). Fig. 1 also depicts the sequence similarity between the NH_2-terminal domain of sheep CD58 and human CD2 as well as human CD48 and human CD2. Human CD48 consists of two Ig-like domains as well (35). As noted, there is considerable homology among the NH_2-terminal domains of the three human CD2 ligands (human CD58, human CD48, and sheep CD58): 55% between human CD58 and sheep CD58 and 30% between human CD58 and human CD48 (Fig. 1). These ligands all possess key conserved Ig domain residues.

Generation and Expression of Human CD58 Mutant Molecules. Residues conserved among at least several of the CD2 ligands seem the most obvious candidates to be implicated in the CD2 contact site. With these criteria in mind, we selected 15 conserved residues in domain 1 which are charged and surface exposed (Fig. 1) for alanine scanning–based site-directed mutagenesis studies. In addition, three charged but nonconserved residues each localized in the predicted C'C" loop, C" and G strands were also mutagenized. As shown in the schematic representation of the human CD58 domain (Fig. 2), 10 of the 18 residues mutated map within β strands:

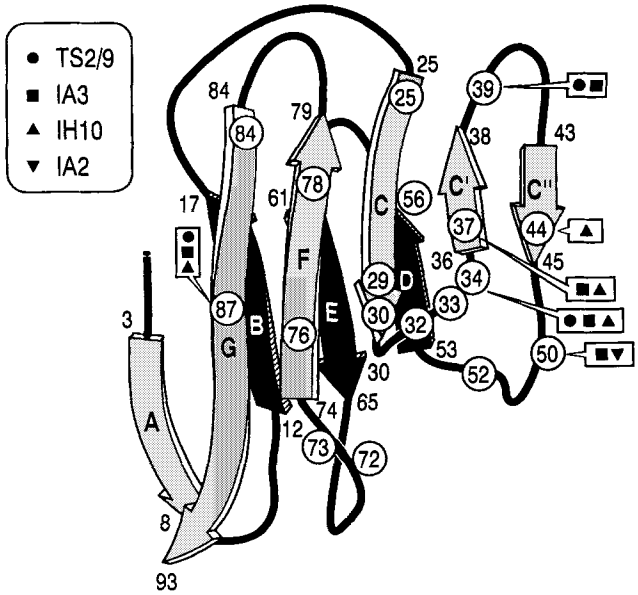

Figure 2. Location of CD58 point mutations and anti-CD58 mAb binding sites on a molecular model of the adhesion domain of human CD58. Ribbon diagram representation of a "MOLSCRIPT" drawing (56, 57) showing the predicted AGFCC'C" β sheet in the front (*light*) and the BED sheet in the back (*dark*) with residue numbers indicating the beginning and end of each β strand. Residues analyzed by site-directed mutagenesis to identify binding sites for CD2 and various anti-CD58 mAbs are shown circled and their positions on the CD58 model, except for P80, are based on both sequence alignment and CD2 β strand assignments (Fig. 1, and 32, 33). Point mutants that affect anti-CD58 mAb binding are indicated with symbols: TS2/9 (●), 1A3 (■), 1H10 (▲), and 1A2 (▼).

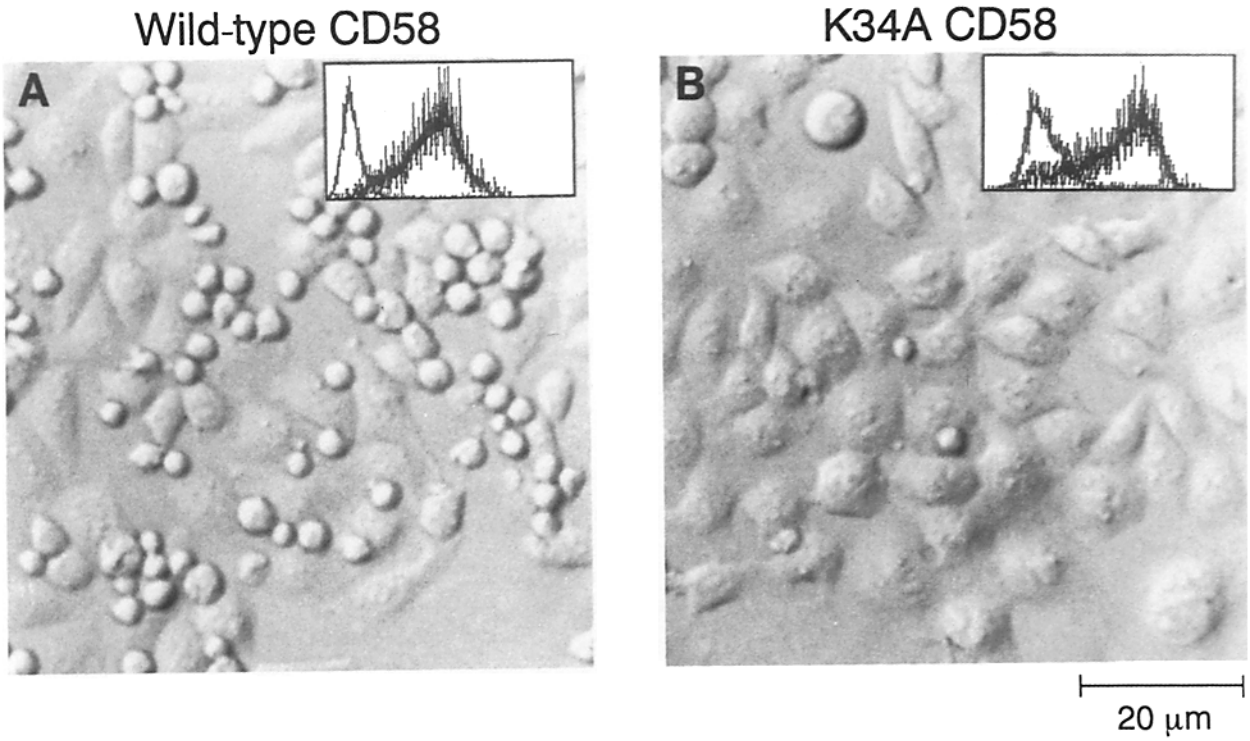

Figure 3. Binding of Jurkat cells to wt or mutant CD58-expressing CHO cells. CHO cells expressing wtCD58 (*A*) or K34A mutant CD58 (*B*) molecules were analyzed for their ability to interact with Jurkat cells and viewed under an inverted phase-contrast microscope (Leitz) at a magnification of 1080. (*Insets*) Fluorescence histograms of 5,000 cells of the indicated CHO transfectants with anti-CD58 (RB202) (*dark curve*) followed by FITC-conjugated goat anti-rabbit Ig or the second antibody alone (*light curve*). (*X-axis*) Mean channel fluorescence over a 4-log scale; (*y-axis*) cell number.

two residues in the G strand (D84 and K87), two residues in the F strand (E76 and E78), three residues in the C strand (E25, K29, and K30), one residue in the C′ strand (E37), one residue in the C″ strand (R44), and one residue in the D strand (D56). The other eight residues tested map within the predicted loops: three residues in the CC′ loop (K32, D33, and K34), one residue in the C′C″ loop (E39), two residues in the C″D loop (K50 and R52), and two residues in the EF loop (E72 and D73). The wtCD58 molecule or individual mutants were transfected into CHO cells and stable lines expressing these molecules were screened by indirect immunofluorescence using a rabbit anti-CD58 heteroantiserum (Rb202). CHO lines expressing CD58 molecules at levels comparable or higher than wtCD58 were selected by immunofluorescence and cell sorting. In this way, we could exclude that loss of CD2 binding activity was related to a low CD58 copy number on the CHO cells.

Specific Cell-based Adhesion Assay to Analyze the Interaction of Human CD2 with CD58 Mutants. The interaction between human CD2 and CD58 was studied in a cell–cell adhesion assay using $CD2^+$ Jurkat cells and CHO cells transfected with CD58 cDNA encoding either wtCD58 or one of the mutant molecules. Previous studies using this assay showed that the binding of Jurkat cells to $CD58^+$ CHO cells is strictly dependent on the CD2–CD58 interaction (24). The photomicrographs in Fig. 3 compare the results of a representative binding experiment between Jurkat and the wtCD58 CHO transfectant on the one hand (Fig. 3 *A*) and between Jurkat and a CD58 point mutant (K34A) which completely disrupts binding on the other hand (Fig. 3 *B*). Note the readily apparent aggregates between the round, relatively small Jurkat cells and the large, fusiform CHO cells transfected with wtCD58. In contrast, virtually no aggregates are formed between Jurkat cells and the K34A CD58 transfectant. This result is noteworthy particularly because the level of CD58 surface expression on K34A CHO transfected cells is more than threefold that on the wtCD58 CHO transfectant (Fig. 3 *insets*, and Table 1).

CD58 Point Mutants. The results of experiments with all CD58 mutants expressed in CHO cells are summarized in Table 1. The percentage of binding for individual CD58 mutants was calculated relative to wtCD58 using a previously described semi-quantitative CHO binding assay with ^{51}Cr-labeled Jurkat cells (24). To exclude the possibility that a loss of CD2 binding capacity was simply a consequence of global disruption of the three-dimensional structure of the CD58 adhesion domain, each mutant was analyzed with a panel of eight anti-CD58 mAbs directed at four distinct native epitopes of the CD58 adhesion domain (termed epitopes 1–4) as defined by prior cross blocking studies (49). The structural integrity of the CD58 adhesion domain point mutants was assessed by reactivity with three mAbs specific for epi-

Table 1. *Summary of Effects of CD58 Mutations on CD2-CD58 Interaction*

CD58 Mutants	Localization of Residue	Level of CD58 Expression	% Binding	anti-CD58 mAb Binding							
				TS2/9	IA3	IH10	IA2	IC4	IC5	IF4	PAK
E25A	C	1.5	68 ± 5	□	□	□	□	□	□	□	□
K29A	C	1.5	35 ± 11	□	□	□	□	□	□	□	□
K30A	C	1.4	64 ± 4	□	□	□	□	□	□	□	□
K32A	CC'	1.5	48 ± 8	□	□	□	□	□	□	□	□
D33A	CC'	2.7	26 ± 6	□	□	□	□	□	□	□	□
K34A	CC'	3.2	1 ± 12	■	■	■	□	□	□	□	□
E37A	C'	1.7	9 ± 7	□	■	■	□	□	□	□	□
E39A	C'C"	2.6	173 ± 3	■	■	□	□	□	□	□	□
R44A	C"	1.3	79 ± 7	□	□	■	□	□	□	□	□
K50A	C"D	1.6	223 ± 4	□	■	□	■	□	□	□	□
R52A	C"D	1.5	125 ± 3	□	□	□	□	□	□	□	□
D56A	D	2.2	159 ± 9	□	□	□	□	□	□	□	□
E72A	EF	1.3	86 ± 7	□	□	□	□	□	□	□	□
D73A	EF	1.9	145 ± 4	□	□	□	□	□	□	□	□
E76A	F	1.4	107 ± 4	□	□	□	□	□	□	□	□
E78A	F	1.9	134 ± 3	□	□	□	□	□	□	□	□
D84A	G	1.4	117 ± 9	□	□	□	□	□	□	□	□
K87A	G	1.4	9 ± 8	■	■	■	□	□	□	□	□

Levels of CD58 expression for the point mutants were compared with wtCD58 and are expressed as a ratio of specific linear mean channel fluorescence intensity of Rb202 heteroantiserum binding to the mutant versus the wt. Percent binding was calculated by taking a ratio of total Jurkat cell binding (average cpm) to each mutant relative to the wtCD58 expressing CHO cells. The standard deviations are shown as a percentage of the total binding. The effect of anti-CD58 mAbs on point mutants were compared with wtCD58 by taking a ratio of the relative mean fluorescence (FL) intensities of mAb binding and Rb202 binding. The reactivities of anti-CD58 mAb binding was calculated as follows: [(FL of mAb binding to mutant − FL of control mAb binding to mutant)/(FL of Rb202 binding to mutant − control sera binding to mutant)]/[(FL of mAb binding to wt − FL of control mAb binding to wt)/(FL of Rb202 binding to wt − FL of control sera binding to wt)]. Reactivities <0.4 are denoted as significant effects (■), and >0.4 as no significant effects (□). Results are representative of a minimum of two experiments for Jurkat cell binding and for mutants that affect mAb binding.

tope 1 (TS2/9, 1A3, and 1H10); one mAb specific for epitope 2 (1A2); three mAbs specific for epitope 3 (1C4, 1C5, and 1F4); and one mAb specific for epitope 4 (PAK). Our results show that epitope 1 and 2 mAbs map to C', C", and G β strands and CC', C'C" and C"D loop regions (Fig. 2, and Table 1). Consistent with the functional evidence that epitope 1 mAbs block E rosette formation, three of the six residues (K87, E37, and K34) to which mAbs TS2/9, 1A3, and 1H10 map are involved in CD2 binding (Table 1). By way of contrast, epitopes 3 and 4 mAbs failed to block the CD58–CD2 interaction and mapped to none of the residues tested on the AGFCC'C" surface. It is thus likely that epitope 3- and 4-specific mAbs map to the BED face of the CD58 adhesion domain or alternatively, to another surface distinct from the CD2 binding region. The epitope 2 mAb cross blocks the binding of both epitopes 1 and 3 (49) and therefore may map to a region that straddles the major β strand surfaces. Our data are consistent with the mapping of 1A2 to the C"D loop (K50). Presumably, the ability of 1A2 to block CD2 binding may be mediated by steric inhibition as the excluded volume of the antibody footprint is large relative to the CD58 adhesion domain. The mutagenesis data herein provide an additional level of refinement to mAb mapping studies as they indicate that even within the epitope 1 group of mAbs, none react with CD58 in precisely the same way (Table 1). The differential effect of CD58 point mutants on mAb binding is evidence that mutations do not cause an overall disruption in the three-dimensional structure of the adhesion domain of CD58. Therefore, we interpret the effects of the CD58 mutants on CD2 binding to be a direct consequence of the mutated residue on CD58.

CD2 Binding Site on CD58. The cellular binding analysis of 18 individual CD58 adhesion domain point mutants expressed in CHO cells identified eight charged residues on the predicted AGFCC'C" surface of the NH_2-terminal CD58 adhesion domain whose mutation to alanine disrupts the binding of $CD2^+$ Jurkat cells. The K34A CHO transfectant binds to Jurkat cells at only 1% the level of the wtCD58 CHO transfectant. In addition, the D33A, E37A, and K87A CD58 mutants show <30% binding to the $CD2^+$ T cells. Four other CD58 point mutants (E25A, K29A, K30A, and K32A) exhibit less dramatic but nonetheless clear-cut effects on CD2 binding (35–68% wt levels). These eight residues on the adhesion domain of CD58 therefore represent potential contact sites for CD2 binding. As shown in Fig. 4, *A* and *B*, it is predicted that their side chains contribute to a charged patch covering a surface area of ~600 $Å^2$ on the AGFCC'C" surface of CD58. It is noteworthy that this surface area is somewhat less than the 770$Å^2$ on the AGFCC'C" face of the CD2 adhesion domain known to be involved in the binding of human CD58 (43). The area is also less than the 650–690$Å^2$ surface contact mediating the homophilic interaction involving the AGFCC'C" surfaces of two rat CD2 molecules in the rat CD2 crystal structure (34). Given that we only probed surface-exposed charged residues on CD58, it is likely that some hydrophobic and/or polar residues may participate in the CD2 binding surface of CD58, thereby contributing to a larger area of contact. For example L27, which

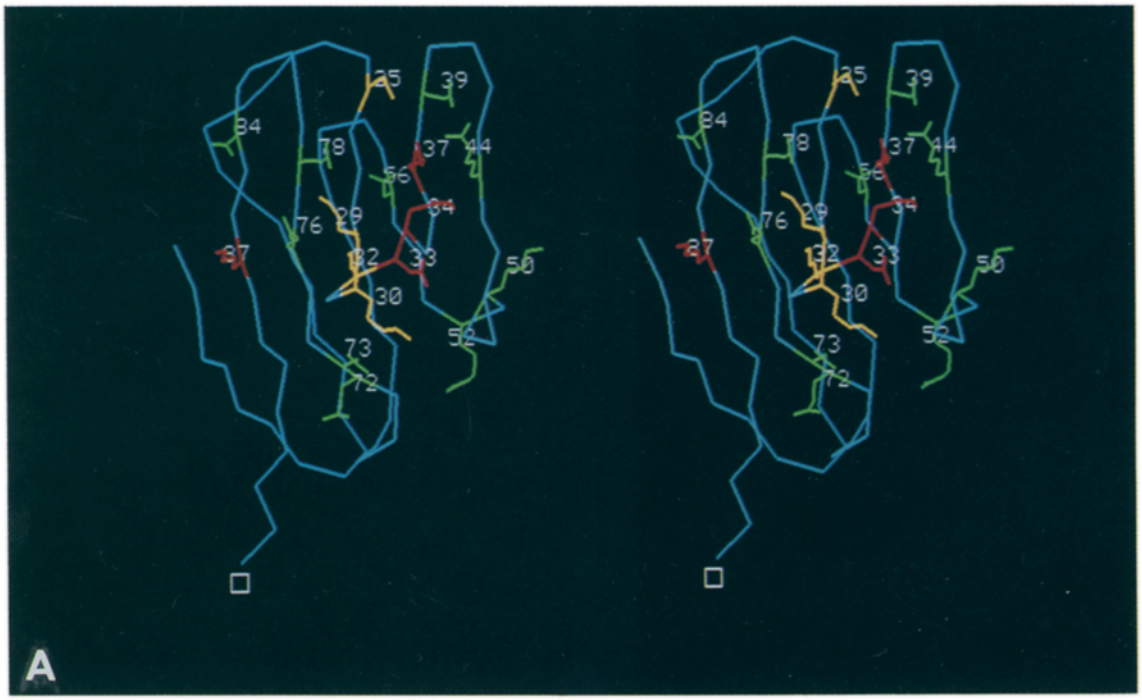
25
39
84
78
37
44
56
34
76
29
87
32
33
50
30
52
73
72
A

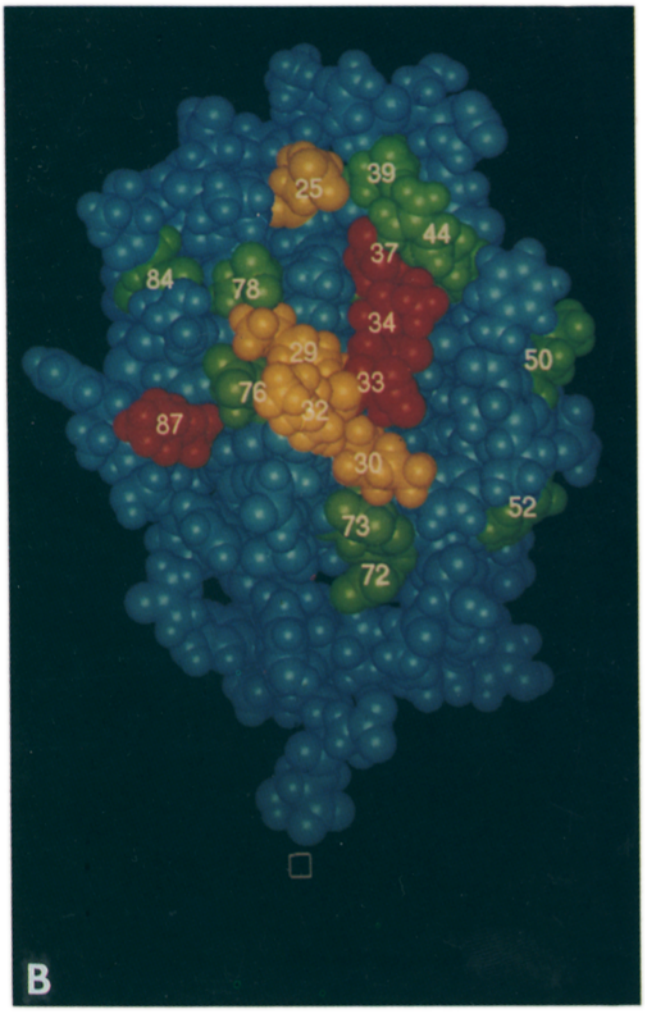
25
39
44
37
84
78
34
29
50
33
76
32
87
30
52
73
72
B

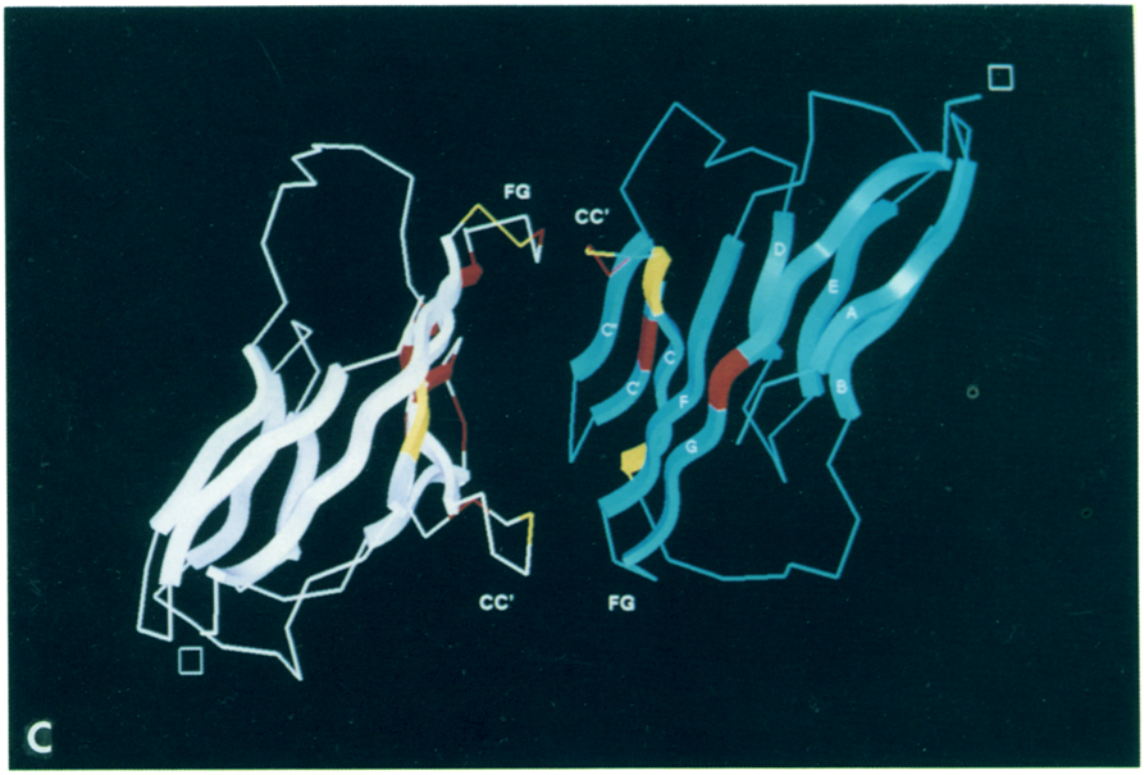
FG
CC'
CC'
FG
C

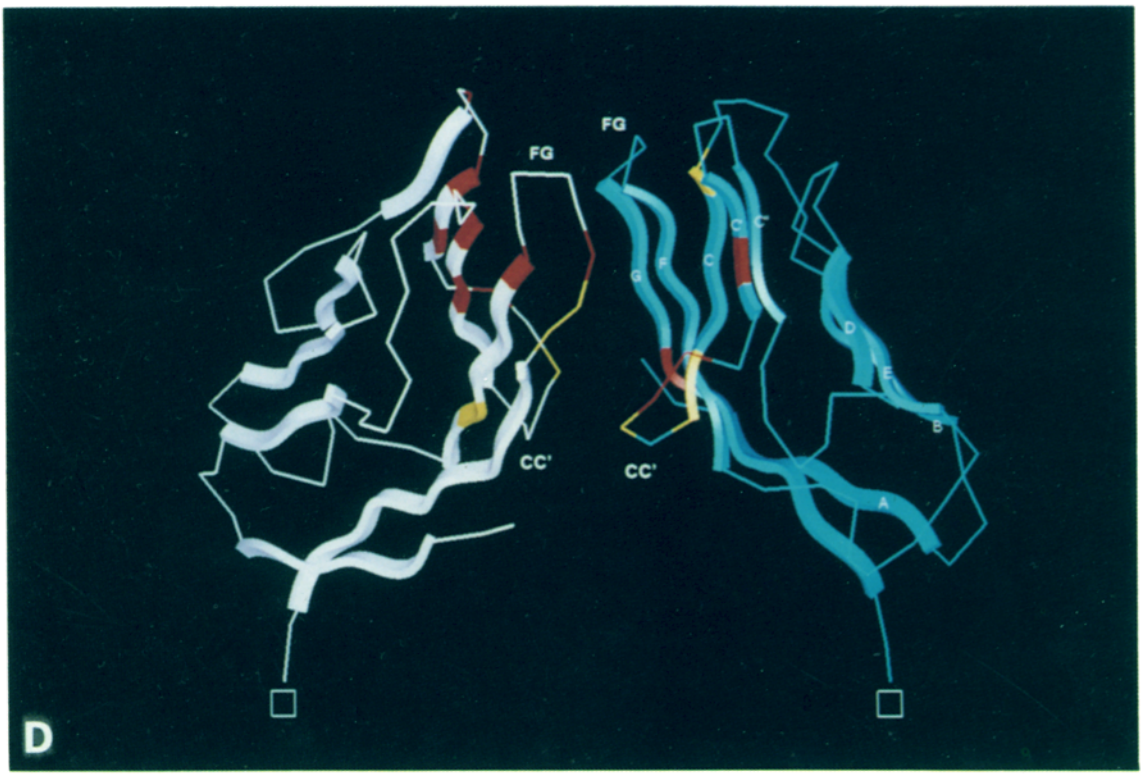
FG
FG
CC'
CC'
D

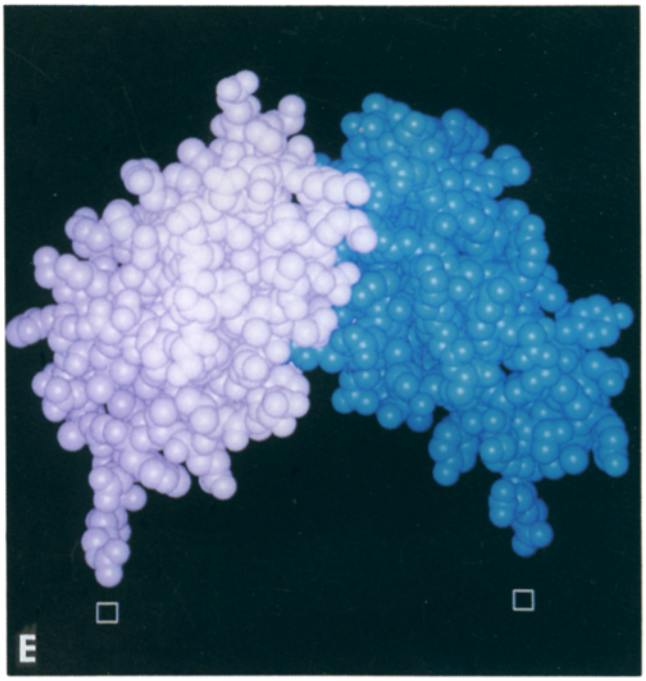

Figure 4. Delineation of the CD2 binding site on CD58 and possible CD2/CD58 docking orientations. The CD2 binding site on CD58 is a highly charged surface area on the predicted AGFCC'C'' surface of the adhesion domain of CD58. Shown is a stereo α-carbon trace model (*A*) and a corresponding space-filling model (*B*). Possible docking orientations for the CD2 (*white*) and CD58 (*blue*) interactions based on the rat CD2 dimer (*C*) or CD8 α homodimer (*D*). A space-filling model for the docking orientation is shown (*E*). Residues on CD58 that showed <30% (*red*) (D*33*, K*34*, E*37*, and K*87*) or 30–75% (*yellow*) (E*25*, K*29*, K*30*, and K*32*) of wt binding to CD2 when substituted with alanine are indicated. Previously defined CD2 residues affecting CD58 binding (43) are also depicted. The COOH-terminal segment of the G strand of the CD58 and CD2 adhesion domain is indicated by an open box.

is predicted to be surface exposed and lies between E25, K29, K34, and E37, may be such a hydrophobic residue (Fig. 4 *B*).

Our results are generally consistent with those of Miller et al. (17) who performed deletional mutagenesis to identify CD58 sequences involved in binding human CD2. Deletion of sequences between residues 11 and 70 on CD58 led to both a loss of CD2 and anti-CD58 mAb binding, whereas deletion of residues 131–180 in the second domain did not affect either CD2 or anti-CD58 mAb binding. However, in contrast to our finding that K87A almost completely abrogated CD2 binding, they reported that a deletion of CD58 residues 71–130 does not affect CD2 binding. Since their result is a negative one, the finding is difficult to interpret especially since another residue in the mutant structure might function in lieu of K87.

Of the four CD58 residues (D33, K34, E37, and K87) that apparently play the greatest role in CD2 binding (<30% wt binding), K34 is conserved among human and sheep CD58, and human CD48 and human CD2 (Fig. 1, and Table 1). Similarly, E37 is conserved in human CD48 and the comparable residue in sheep CD58 and human CD2 is the related amino acid glutamine. K87 is also conserved between human CD58 and CD48. In view of the conservation of K34, E37, and K87 in human CD58 and CD48 and their observed functional effects on the CD2–CD58 interaction, it is likely that the corresponding residue in CD48 is involved in the CD2 interaction. If this is so, CD48 and CD58 may bind to CD2 in a similar way. In contrast, the other five charged CD58 residues (E25, K29, K30, K32, and D33) which contribute to CD2 binding, are conserved between human and sheep variants of CD58 but not human CD48. These residues may, at least in part, be responsible for the higher affinity of the CD58 interaction with human CD2 (K_d $\sim 10^{-6}$ M) relative to the human CD48 interaction with human CD2 (K_d $\sim 10^{-4}$ M). Polar and/or hydrophobic residues yet to be identified may also contribute to the higher-affinity interaction between CD2 and CD58. Collectively, these data also suggest that human and sheep CD58 interact with CD2 in a similar manner, consistent with our prior analysis of mutant CD2 molecules (43). In that study, it was observed that CD2 mutations which disrupted the sheep CD58 interaction also disrupted the human CD58 interaction.

Possible Docking Orientation of CD58 and CD2. The mutational data for CD58 presented herein and for CD2 presented elsewhere (43) define the area of interaction between these proteins. To develop a model of the CD2–CD58 complex, we considered as paradigms several examples of crystallographically defined docking orientations between Ig-related molecules. These include the known interaction between Ig V_H and V_L domains, between human CD8 α subunits in the CD8 α-α homodimer and between two CD2 molecules in the rat CD2 crystal structure (34, 46, 47). Since the packing between CD8 α subunits is close to that between V_H and V_L, the latter were not studied separately. However, the orientation of molecules in the rat CD2 dimer structure is distinct from that of CD8 or Ig dimers (34). In the CD8 α-α homodimer structure, the molecular association between subunits involves main chain hydrogen bonding between the C' strand of one molecule and the G strand of the other. In the rat CD2 dimer, the CC' and FG loops are shortened compared to CD8, and the relative orientations of their domains differ by ~60° from that of CD8. This reduces the extent of the hydrogen bonding interaction to the beginning of the C' and G strands where they join the CC' and FG loops, respectively.

Based on these examples, two possible docking orientations for the CD58–CD2 interaction were created. The first docking orientation (Fig. 4 *C*) was constructed using a model of the rat CD2 dimer: one rat CD2 adhesion domain was replaced by the human CD2 NMR structure by least squares superimposition of the C_α atoms of residues in the binding sheet and the other domain substituted by the human CD58 model. As shown in Fig. 4 *C*, this orientation brings the FG and CC' loop of CD2 and CD58 adjacent to each other. In this docking orientation, the COOH-terminal end of the G strands of CD2 and CD58 point away from each other in essentially opposite directions, presumably towards two separate cell membranes. Fig. 4 *D* represents a second pos-

sible docking orientation based on the coordinates of the CD8 α homodimer which bring the FG loops of CD2 and CD58 near one another as shown. If this orientation is correct, then the COOH-terminal segments of the G strand in CD2 and CD58 are only separated by an angle of $\sim$60°. Given that the crystal structure of the two domain rat CD2 molecule identifies an angle of $\sim$160° between the adhesion domain of CD2 and the second domain plus COOH-terminal stalk region (34), it is plausible that the adhesion domains of CD2 and CD58 could approach one another from two separate cell membranes in such a manner.

Both docking models take into account all the side chains implicated in binding with one exception. In the CD2 dimer–based model (Fig. 4 *C*), K87 on CD58, which is involved in CD2 binding, is an outlier and makes no contacts with CD2. In contrast, in the CD8α-based model (Fig. 4 *D*), it is on the edge of the binding interface and can be involved in direct interaction. This difference tends to support the CD8α-based model as more representative of the real CD2–CD58 docking orientation. On the other hand, our efforts at de novo docking of CD2 and CD58 suggest an orientation close to the CD2 dimer–based model that readily provides K87 with contacts to CD2 (data not shown). Hence, we cannot make a definitive statement about the docking orientations of CD2 and CD58 at present. A space-filling model of the CD2–CD58 interaction in the CD8-based orientation (Fig. 4 *E*) shows that the nature of the contact surface size and shape is also reasonable.

Implications for the CD2–CD58 Interaction. Our prior mutagenesis analysis shows that the CD58 binding site on CD2 covers $\sim$770Å^2 on the AGFCC'C'' face of the CD2 β barrel (43). This site contains β strand residues in the COOH-terminal half of the F strand (including K82 and Y86), the top of the C strand (D32 and K34), and the C' strand (Q46), which are all solvent exposed. In addition, several exposed residues on the FG loop (G90, K91, N92, and V93), the CC' loop (K41 and K43) and the C'C'' loop (R48 and K51) form this site. The current mutagenesis on CD58 has uncovered the other surface of the interaction involving five positively charged residues (K29, K30, K32, K34, and K87) and three negatively charged residues (E25, D33, and E37). In light of the seven positively charged and one negatively charged CD2 residues involved in this site, it appears there is an excess of positive charge. This excess positive charge may be satisfied by interaction with water. Alternatively, the positive charge may also be satisfied by negatively charged side chains that appear not to be crucial for binding (E39, E76, and E78) or are near the site (E42 and E74) but whose contribution to CD2 binding is yet to be determined. The ability of sulfated dextrans to inhibit the CD2–CD58 interaction is probably a consequence of direct binding of these polymers to the positively charged CD2 and/or CD58 surface (50).

The mapping of the CD2 binding site to the predicted AGFCC'C'' surface of the CD58 adhesion domain shows that the major β sheet surfaces mediating interaction between CD2 and CD58 are the same as those mediating dimerization of other Ig-variable domains including Ig, CD8α, and rat CD2 (34, 46, 47). In the CD8α homodimer and V_H–V_L interactions, the G and C' strands contain conserved β bulges located at the dimer interface which are believed to facilitate dimerization (47, 51, 52). The CD58 residue E37 on the predicted C' strand and residues K32, D33, and K34 adjacent to the start of this strand and K87 within the predicted G strand are all important for CD2 binding. These residues may actually be components of equivalent β bulges. Support for this notion is the finding that the corresponding residue in the CD2 C' strand (Q46) and residues adjacent to this (K41 and K43) are critical for CD58 binding (43, 53). They are located on the corresponding β bulge of CD2 (32, 33). Mutations of G90, K91, N92, and V93 near the start of the CD2 G strand disrupt CD58 binding but there is no evidence for a β bulge in the G strand (33). The prevalence of charged residues in the predicted CD2–CD58 interface noted above appears to differ from the predominant hydrophobic interaction among residues found at the site of V_H-V_L domain packing (51). However, if there is a β bulge located in the G strand of CD58 involving residues K87, F88, and F89, then this bulge would expose hydrophobic side chains that would involve hydrophobic contacts between CD2 and CD58.

The present analysis of the molecular interface in the CD2–CD58 complex offers a first consideration of the nature of a receptor-ligand pair involving two Ig supergene family members. Such interactions are distinct from those between V domains in idiotype–anti-idiotype complexes where major surface contacts are mediated via the CDR1 (BC), CDR2 (C'C''), and CDR3 (FG) loops (54, 55). They are also different from the interaction between Ig constant region domains which involve the BED β sheet surface (57). Given that either of the two CD2-CD58 docking orientations might facilitate conjugate formation between T lymphocytes and APCs, the precise orientation of the interaction awaits elucidation by structural analysis of a CD2–CD58 complex. Alternatively, it may be possible to infer the correct docking mode by further mutagenesis involving reciprocal charge reversals in CD2 and CD58.

We thank Dr. Tetsu Kakutani for supplying the sheep CD58 sequence prior to submission to the DDBJ DNA data base; Dr. Laurelee Osborn for providing the Rb202 anti-CD58 hetero anti-sera; Drs. Stefan Meuer and Ulrich Moebius for providing anti-CD58 mAbs; Dr. Reinhard Wallich for sharing unpublished information on genomic cloning of CD58; and Dr. Per Kraulis for the "MOLSCRIPT" program. We also acknowledge Ms. Yasmin Hussain for oligonucleotide synthesis and Mr. Peter Lopez and members of the core flow cytometry facility for flow cytometric analysis.

This work was supported by National Institutes of Health grants AI-21226 to E. L. Reinherz and GM-38608 to G. Wagner.

Address correspondence to Dr. A. R. N. Arulandandam, Laboratory of Immunobiology, Dana-Farber Cancer Institute, 44 Binney Street, Boston, MA 02135.

Received for publication 25 May 1994 and in revised form 15 July 1994.

References

1. Moingeon, P., H.-C. Chang, P.H. Sayre, L.K. Clayton, A. Alcover, P. Gardner, and E.L. Reinherz. 1989. The structural biology of CD2. *Immunol. Rev.* 111:111.
2. Springer, T.A. 1990. Adhesion receptors of the immune system. *Nature (Lond.).* 346:424.
3. Bierer, B.E., B.P. Sleckman, S.E. Ratnofsky, and S.J. Burakoff. 1989. Biologic roles of CD2, CD4 and CD8 in T cell activation. *Annu. Rev. Immunol.* 7:579.
4. Moingeon, P., H.-C. Chang, B.P. Wallner, C. Stebbins, A.Z. Frey, and E.L. Reinherz. 1989. CD2-mediated adhesion facilitates T lymphocyte antigen recognition function. *Nature (Lond.).* 339:312.
5. Koyasu, S., T. Lawton, D. Novick, M.A. Recny, R.F. Siliciano, B.P. Wallner, and E.L. Reinherz. 1990. Role of interaction of CD2 molecules with lymphocyte function associated antigen 3 in T cell recognition of nominal antigen. *Proc. Natl. Acad. Sci. USA.* 87:2603.
6. Meuer, S.C., R.E. Hussey, M. Fabbi, D. Fox, O. Acuto, K.A. Fitzgerald, J.C. Hodgdon, J.P. Protentis, S.F. Schlossman, and E.L. Reinherz. 1984. An alternative pathway of T cell activation: a functional role for the 50 KD T11 sheep erythrocyte receptor protein. *Cell.* 36:897.
7. Yang, S.-Y., S. Chouaib, and B. Dupont. 1986. A common pathway for T lymphocyte activation involving both the CD3-Ti complex and CD2 sheep erythrocyte receptor determinants. *J. Immunol.* 137:1097.
8. Hünig, T., G. Tiefenthaler, K.-H. Meyer zum Büschenfelde, and S.C. Meuer. 1987. Alternative pathway activation of T cells by binding of CD2 to its cell surface ligand. *Nature (Lond.).* 326:298.
9. Bierer, B.E., A. Peterson, J.C. Gorga, S.H. Herrmann, and S.J. Burakoff. 1988. Synergistic T cell activation via the physiological ligands for CD2 and the T cell receptor. *J. Exp. Med.* 168:1145.
10. Chang, H.-C., P. Moingeon, P. Lopez, H. Krasnow, C. Stebbins, and E.L. Reinherz. 1989. Dissection of the human CD2 intracellular domain. Identification of a segment required for signal transduction and interleukin 2 production. *J. Exp. Med.* 169:2073.
11. He, Q., A.D. Beyers, A.N. Barclay, and A.F. Williams. 1988. A role in transmembrane signalling for the cytoplasmic domain of the CD2 T lymphocyte surface antigen. *Cell.* 54:979.
12. Siliciano, R.F., J.C. Pratt, R.E. Schmidt, J. Ritz, and E.L. Reinherz. 1985. Activation of cytolytic T lymphocytes and natural killer cell function through the T11 sheep erythrocyte binding protein. *Nature (Lond.).* 317:428.
13. Arulanandam, A.R.N., S. Koyasu, and E.L. Reinherz. 1991. T cell receptor–independent CD2 signal transduction in FcR^+ cells. *J. Exp. Med.* 173:859.
14. Moingeon, P., J.L. Lucich, D.J. McConkey, F. Letourneur, B. Malissen, J. Kochan, H.-C. Chang, H.-R. Rodewald, and E.L. Reinherz. 1992. CD3 ζ dependence of the CD2 pathway of activation in T lymphocytes and natural killer cells. *Proc. Natl. Acad. Sci. USA.* 89:1492.
15. Sayre, P.H., R.E. Hussey, H.-C. Chang, T.L. Ciardelli, and E.L. Reinherz. 1989. Structural and binding analysis of a two domain extracellular CD2 molecule. *J. Exp. Med.* 169:995.
16. Recny, M.A., E.A. Neidhardt, P.H. Sayre, T.L. Ciardelli, and E.L. Reinherz. 1990. Structural and functional characterization of the CD2 immunoadhesion domain. *J. Biol. Chem.* 265:8542.
17. Miller, G.T., P.S. Hochman, W. Meier, R. Tizard, S.A. Bixler, M.D. Rosa, and B.P. Wallner. 1993. Specific interaction of lymphocyte function-associated antigen 3 with CD2 can inhibit T cell responses. *J. Exp. Med.* 178:211.
18. Moingeon, P., J.L. Lucich, C.C. Stebbins, M.A. Recny, B.P. Wallner, S. Koyasu, and E.L. Reinherz. 1991. Complementary roles for CD2 and LFA-1 adhesion pathways during T cell activation. *Eur. J. Immunol.* 21:605.
19. Tiefenthaler, G., M.L. Dustin, T.A. Springer, and T. Hunig. 1987. Serologic crossreactivity of T11 target structure and lymphocyte function–associated antigen 3. *J. Immunol.* 139:2696.
20. Lay, W.H., N.F. Mendes, C. Bianco, and V. Nussenzweig. 1971. Binding of sheep red blood cells to a large population of human lymphocytes. *Nature (Lond.).* 230:531.
21. Brain, P., J. Gordon, and W.A. Willetts. 1970. Rosette formation by peripheral lymphocytes. *Clin. Exp. Immunol.* 6:681.
22. Coombs, R.R.A., R.W. Burner, A.B. Wilson, G. Holm, and B. Lindgren. 1970. Rosette-formation between human lymphocytes and sheep red cells not involving immunoglobulin receptors. *Int. Arch. Allergy Appl. Immunol.* 39:658.
23. Jondal, M., G. Holm, and H. Wigzell. 1972. Surface markers on human T and B lymphocytes: a large population of lymphocytes forming nonimmune rosettes with sheep red blood cells. *J. Exp. Med.* 136:207.
24. Arulanandam, A.R.N., P. Moingeon, M.F. Concino, M.A. Recny, K. Kato, H. Yagita, S. Koyasu, and E.L. Reinherz. 1993. A soluble multimeric recombinant CD2 protein identifies CD48 as a low affinity ligand for human CD2: divergence of CD2 ligands during the evolution of humans and mice. *J. Exp. Med.* 177:1439.
25. Kato, K., M. Koyanagi, H. Okada, T. Takanashi, Y.-W. Wong, A.F. Williams, K. Okumura, and H. Yagita. 1992. CD48 is a counter-receptor for murine CD2 and is involved in T cell activation. *J. Exp. Med.* 176:1241.
26. Sayre, P.H., H.-C. Chang, R.E. Hussey, N.R. Brown, N.E. Richardson, G. Spagnoli, L.K. Clayton, and E.L. Reinherz. 1987. Molecular cloning and expression of T11 cDNAs reveal a receptor-like structure on human T lymphocytes. *Proc. Natl. Acad. Sci. USA.* 84:2941.

27. Seed, B., and A. Aruffo. 1987. Molecular cloning of the CD2 antigen, the T cell erythrocyte receptor, by a rapid immunoselection procedure. *Proc. Natl. Acad. Sci. USA.* 84:3365.
28. Seed, B. 1987. An LFA-3 cDNA encodes a phospholipid-linked membrane protein homologous to its receptor CD2. *Nature (Lond.).* 329:840.
29. Wallner, B.P., A.Z. Frey, R. Tizard, R.J. Mattaliano, C. Hession, M.E. Sanders, M.L. Dustin, and T.A. Springer. 1987. Primary structure of lymphocyte function-associated antigen (LFA-3): the ligand of the T lymphocyte CD2 glycoprotein. *J. Exp. Med.* 166:923.
30. Williams, A.F., and A.N. Barclay. 1987. The immunoglobulin superfamily - domains for cell surface recognition. *Annu. Rev. Immunol.* 6:381.
31. Driscoll, P.C., J.G. Cyster, I.D. Campbell, and A.F. Williams. 1991. Structure of domain 1 of rat T lymphocyte CD2 antigen. *Nature (Lond.).* 353:762.
32. Withka, J.M., D.F. Wyss, G. Wagner, A.R.N. Arulanandam, E.L. Reinherz, and M.A. Recny. 1993. Structure of the glycosylated adhesion domain of human T lymphocyte glycoprotein CD2. *Structure.* 1:69.
33. Wyss, D.F., J.M. Withka, M.H. Knoppers, K.A. Sterne, M.A. Recny, and G. Wagner. 1993. ^{1}H Resonance assignments and secondary structure of the 13.6 KDa glycosylated adhesion domain of human CD2. *Biochemistry.* 32:10995.
34. Jones, E.Y., S.J. Davis, A.F. Williams, K. Harlos, and D.I. Stuart. 1992. Crystal structure at 2.8Å resolution of a soluble form of the cell adhesion molecule CD2. *Nature (Lond.).* 360:232.
35. Staunton, D.E., and D.A. Thorley-Lawson. 1987. Molecular cloning of the lymphocyte activation marker Blast-1. *EMBO (Eur. Mol. Biol. Organ.) J.* 6:3695.
36. Staunton, D.E., R.C. Fisher, M.M. LeBeau, J.B. Lawrence, D.E. Barton, U. Francke, M. Dustin, and D.A. Thorley-Lawson. 1989. Blast-1 possesses a glycosyl-phosphatidylinositol (GPI) membrane anchor, is related to LFA-3 and OX-45, and maps to chromosome 1q21-23. *J. Exp. Med.* 169:1087.
37. Sewell, W.A., R.W. Palmer, N.K. Spurr, D. Sheer, M.H. Brown, Y. Bell, and M.J. Crumpton. 1988. The human LFA-3 gene is located at the same chromosome band as the gene for its receptor CD2. *Immunogenetics.* 28:278.
38. Wong, Y.W., A.F. Williams, S.F. Kingsmore, and M.F. Seldin. 1990. Structure, expression, and genetic linkage of the mouse BCM1 (OX45 or Blast-1) antigen: evidence for genetic duplication giving rise to the BCM1 region on mouse chromosome 1 and the CD2/LFA3 region on mouse chromosome 3. *J. Exp. Med.* 171:2115.
39. Diamond, D.J., L.K. Clayton, P.H. Sayre, and E.L. Reinherz. 1988. Exon-intron organization and sequence comparison of human and murine T11 (CD2) genes. *Proc. Natl. Acad. Sci. USA.* 85:1615.
40. Krensky, A.M., F. Sanchez-Madrid, E. Robbins, J.A. Nagy, T.A. Springer, and S.J. Burakoff. 1983. The functional significance, distribution and structure of LFA-1, LFA-2 and LFA-3: cell surface antigens associated with CTL-target interactions. *J. Immunol.* 131:611.
41. Yokoyama, S., D. Staunton, R. Fisher, M. Amiot, J.J. Forin, and D.A. Thorley-Lawson. 1991. Expression of the Blast-1 activation/adhesion molecule and its identification as CD48. *J. Immunol.* 146:2192.
42. Reinherz, E.L., and S.F. Schlossman. 1980. The differentiation and function of human T lymphocytes. *Cell.* 19:821.
43. Arulanandam, A.R.N., J.M. Withka, D.F. Wyss, G. Wagner, A. Kister, P. Pallai, M.A. Recny, and E.L. Reinherz. 1993. The CD58 (LFA-3) binding site is a localized and highly charged surface area on the AGFCC'C'' face of the human CD2 adhesion domain. *Proc. Natl. Acad. Sci. USA.* 90:11613.
44. Somoza, C., P.C. Driscoll, J.G. Cyster, and A.F. Williams. 1993. Mutational analysis of the CD2/CD58 interaction: the binding site for CD58 lies on one face of the first domain of human CD2. *J. Exp. Med.* 178:549.
45. Dengler, T.J., J.C. Hoffmann, P. Knolle, M.A.-Wolf, M. Roux, R. Wallich, and S.C. Meuer. 1992. Structural and functional epitopes of the human adhesion receptor CD58 (LFA-3). *Eur. J. Immunol.* 22:2809.
46. Epp, O., E.E. Lattman, M. Schiffer, and R. Huber. 1975. The molecular structure of a dimer composed of the two variable portions of the Bence-Jones protein/REI. *Biochemistry.* 14:4943.
47. Leahy, D.J., R. Axel, and W. Hendrickson. 1992. Crystal structure of a soluble form of the human T cell coreceptor CD8 at 2.6 Å resolution. *Cell.* 68:1145.
48. Wang, J., Y. Yan, T.P.J. Garrett, J. Liu, D.W. Rodgers, R.L. Garlick, G.E. Tarr, Y. Hussain, E.L. Reinherz, and S.C. Harrison. 1990. Atomic structure of a fragment of human CD4 containing two immunoglobulin-like domains. *Nature (Lond.).* 348:411.
49. Gray, F., J.G. Cyster, A. Willis, A.N. Barclay, and A.F. Williams. 1993. Structural analysis of the CD2 T lymphocyte antigen by site-directed mutagenesis to introduce a disulphide bond into domain 1. *Protein Eng.* 6:965.
50. Parish, C.R., V. McPhun, and H.S. Warren. 1988. Is a natural ligand of the T lymphocyte CD2 molecule a sulfated carbohydrate? *J. Immunol.* 141:3948.
51. Chothia, C., J. Novotny, R. Bruccoleri, and M. Karplus. 1985. Domain association in immunoglobulin molecules: the packing of variable domains. *J. Mol. Biol.* 186:651.
52. Colman, P.M. 1988. Structure of antibody-antigen complexes: implications for immune recognition. *Adv. Immunol.* 43:99.
53. Peterson, A., and B. Seed. 1987. Monoclonal antibody and ligand binding sites of the T cell erythrocyte receptor (CD2). *Nature (Lond.).* 329:842.
54. Bentley, G.A., G. Boulot, M.M. Riottot, and R.J. Poljak. 1990. Three-dimensional structure of an idiotope-anti-idiotope complex. *Nature (Lond.).* 348:254.
55. Ban, N., C. Escobar, R. Garcia, K. Hasel, J. Day, A. Greenwood, and A. McPherson. 1994. Crystal structure of an idiotype-anti-idiotype Fab complex. *Proc. Natl. Acad. Sci. USA.* 91:1604.
56. Kraulis, P.J. 1991. MOLSCRIPT: a program to produce both detailed and schematic plots of protein structures. *J. Applied Crystallography.* 24:946.
57. Edmunson, A.B., K.R. Ely, E.E. Abola, M. Schiffer, and N. Panagiotopoulous. 1975. Rotational allomerism and divergent evolution of domains in Ig light chains. *Biochemistry.* 14:3953.